02

A quantum capacitance of the graphene/$Li_3V_2(PO_4)_3$ composite during delithiation

© V.V. Shunaev, A.A. Petrunin, A.V. Ushakov, O.E. Glukhova

Saratov National Research State University,
410012 Saratov, Russia
e-mail: vshunaev@list.ru

Received December 25, 2023
Revised December 25, 2023
Accepted December 25, 2023

By the *ab initio* method, the electron-energy structure of the graphene/$Li_3V_2(PO_4)_3$ composite with different mass concentrations was studied. The structures of the composite were explored with the step-by-step extraction of lithium from the supercell of the composite, which simulates its states during the charging of the electrode material. For each stage of delithiation, the distribution of quantum capacitance as a function of the applied voltage was calculated. Based on the analysis of these distributions, it was proposed an approach for estimating the dependence of the accumulated quantum capacitance taking into account changes in composition, which simulates the charging curve in real experiments. The obtained results allow us to draw conclusions about the nature of the quantum capacitance and its relationship with the charge/discharge curves of the electrodes of lithium-ion batteries.

Keywords: lithium-ion batteries, quantum capacitance, lithium phosphate, graphene, ab initio.

DOI: 10.21883/0000000000

Introduction

High energy density and durability make lithium-ion batteries (LIB) central to the development of chemical power sources. Vanadium-lithium phosphate $Li_3V_2(PO_4)_3$ is a promising cathode material because it has a high oxidation-reduction potential, good electrochemical and thermodynamic stability, high speed of the electrode process, as well as the highest theoretical capacity (197 mA·h/g) among phosphates [1–5]. The combination of vanadium-lithium phosphate with carbon superconducting structures (graphene, graphene oxide, carbon nanotubes) allows to achieve this capacity, as well as increase the mechanical stability of the material [6,7]. It is known that in low-dimensional materials, the contribution to the total capacity of the C_T structure is made by the capacity of the double electric layer C_D and the quantum capacitance C_Q, reflecting changes in the charge in the structure with a shift in the Fermi level [8–10]:

$$\frac{1}{C_T} = \frac{1}{C_Q} + \frac{1}{C_D}. \qquad (1)$$

Thus, analysis of the quantum capacitance of cathode materials is an urgent task, the solution of which can be an important step towards improving LIB. The purpose of this *ab initio* study is to construct atomic supercells of the $Li_3V_2(PO_4)_3$/graphene (hereinafter — LVP/G) composite) with different mutual mass concentrations of components, followed by analysis of the dependence of the quantum capacitance on the applied voltage. Besides, as part of this work, an attempt will be made for the first time to analyze the quantum capacitance of the LVP/G composite during the delithiation process.

1. Experimental

Atomistic modeling of the structures under study was carried out using the DFT (Density Functional Theory) method as part of the gradient approximation (GGA) with the exchange and correlation functional in the PBE version (Perdew, Burke, Ernzerhof) in the Siesta [11] software package. Dispersion interactions were taken into account by the Grimme correction DFT-D2. The Li, P, V atoms were modeled in the DZP basis, while the O and C atoms — were modeled in the lightweight DZ basis. This is due to the fact that taking into account polarization orbitals by the DZP basis for atoms O and C contributes only 0.7% to the total charge of the atom, and for atoms Li, P, V — approximately 25%. Integration over the irreducible part of the Brillouin zone was performed by Monkhorst −Puck method on grids of k points, $2 \times 2 \times 2$ for $3D$ structures and $6 \times 6 \times 1$ for $2D$ films. The strength convergence did not exceed 0.05 eV/Å. The density of electronic states (DOS) plot was constructed based on the eigenvalue matrix obtained by solving the stationary Schrodinger equation. When constructing the DOS, Gaussian distributions with a broadening of 0.01 were used.

The bond energy between graphene and phosphate was calculated using the formula

$$E_B(G/LVP) = E(G + LVP) - E(G) - E(LVP), \qquad (1)$$

where E(G+LVP) — energy of the composite, E(G) — energy of graphene, E(LVP) — energy of phosphate in an isolated state.

Quantum capacitance, [F/g], for a stationary structure depending on the applied voltage V, [V], corresponding to

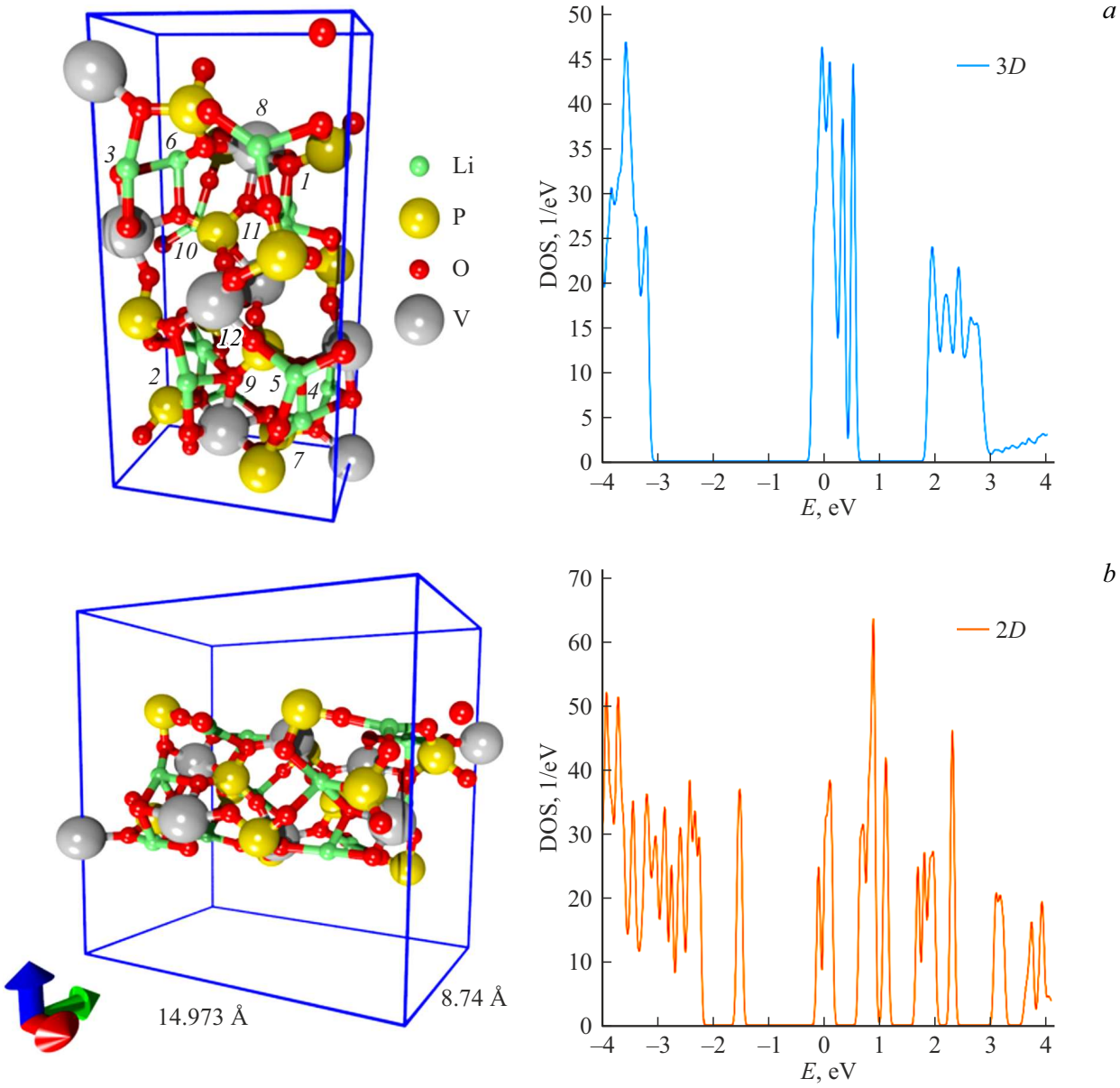

Figure 1. Unit cells $Li_3V_2(PO_4)_3$ and corresponding DOS graphs: *a* —3*D*–; *b* — 2*D*-film.

the Fermi level shift E_F, can be obtained based on the graph of the density of electronic states (DOS):

$$C_Q(V) = \frac{1}{mV}\int_0^V eD(E_F - eV')dV', \qquad (2)$$

where m — mass of the structure [g], D — area under the DOS graph in the considered energy range [eV^{-1}·eV], e — elementary charge [C].

To model the charging curve (the dependence of capacity on potential), let us review the dependence of quantum capacitance on the degree of lithium extraction using the following method. Let E_{F0} — Fermi level corresponding to the initial state of the structure (with the initial number of lithium atoms N). The structure with the number of lithium atoms N_i and the Fermi level E_{Fi} corresponds to the voltage $U_i = (E_{F0} - E_{Fi})e$. The value of the quantum capacitance at 0 V (at the Fermi level) for this structure will be denoted by C_Q^0 (U_i). The additional integral quantum capacitance, which corresponds to the charge accumulation by the electrode, at each step of the extraction of lithium atoms $\Delta Q(U_i)$ can be calculated as the average value between the quantum capacitances at the Fermi level $C_Q^0(U_i)$ and $C_Q^0(U_{i-1})$, multiplied by the voltage increment $|U_i - U_{i-1}|$.

$$\Delta Q(U_i) = \frac{C_q^0(U_i) + C_q^0(U_{i-1})}{2}|U_i - U_{i-1}|. \qquad (3)$$

The accumulated quantum capacitance, taking into account the change in composition from the initial one at

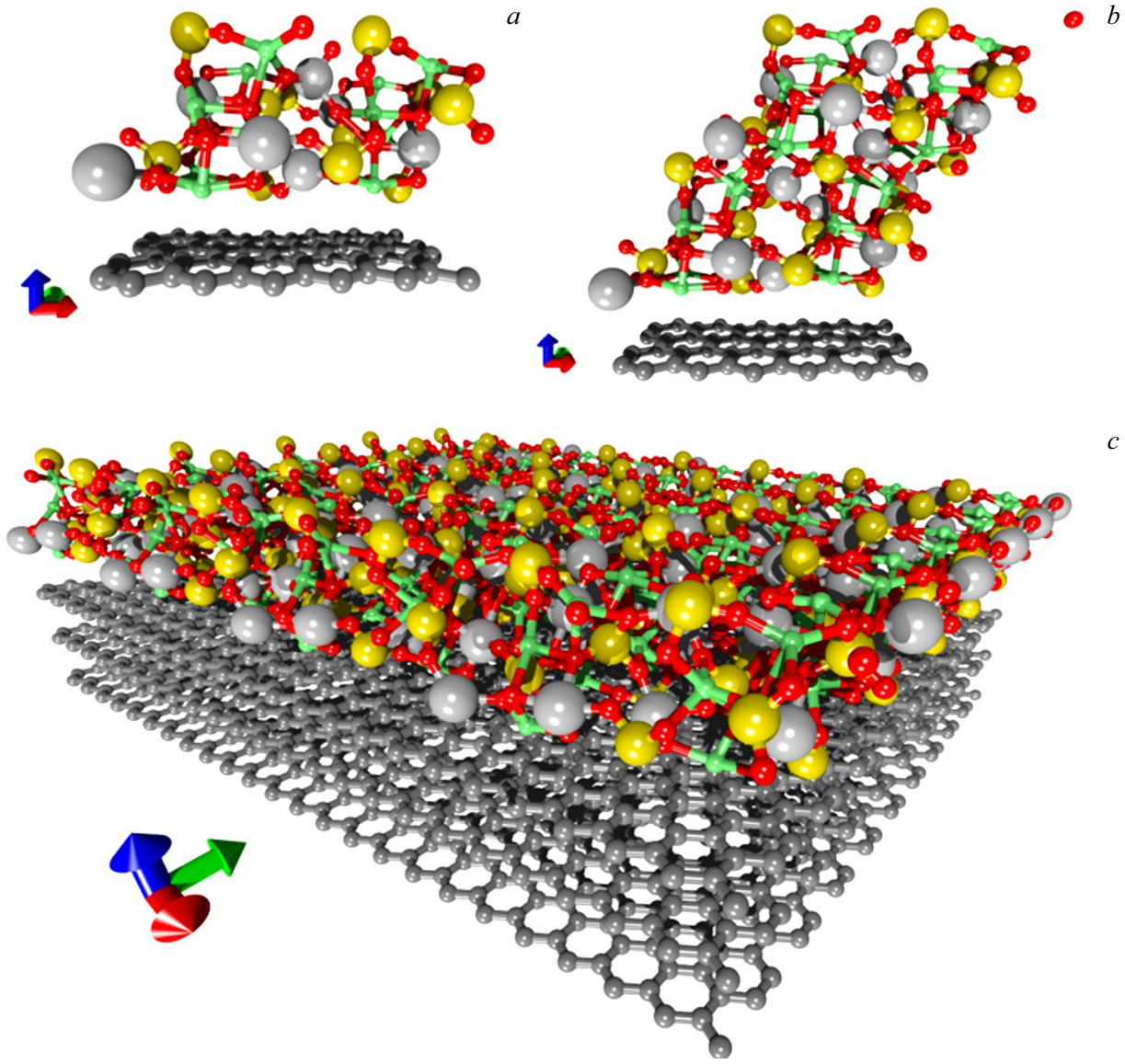

Figure 2. Supercells of LVP/G composites with mass ratio m($Li_3V_2(PO_4)_3$): m(graphene): *a* — 3 : 1; *b* — 6 : 1; *c* — 1 : 1 (supercell expanded in two directions).

voltage U_i (in C/g), can be found using the cumulative formula:

$$Q(U_i) = Q(U_{i-1}) + \Delta Q(U_i). \quad (4)$$

Meanwhile, we believe that $Q(0) = 0$. Converting the value from units [C/g] to units of specific capacity [mA·h/g] accepted for chemical current sources is done by dividing by $\left(Q\left[\frac{mA \cdot h}{g}\right] = Q\left[\frac{C}{g}\right] \cdot 1000\left[\frac{mA}{A}\right]\frac{1}{3600}\left[\frac{h}{s}\right]\right)$

2. Findings

The lattice cell $Li_3V_2(PO_4)_3$, containing 8 vanadium atoms, 12 lithium atoms, 12 phosphorus atoms, is shown in Fig. 1, *a*, on the left. This cell corresponds to the monoclinic symmetry group P21/c, which is known to be the most thermodynamically stable for this substance [2,4]. The DOS of the cell $Li_3V_2(PO_4)_3$, translated in three directions, is shown in Fig. 1, *a*, on the right. As can be seen from the graph, the 3*D*-cell $Li_3V_2(PO_4)_3$ demonstrates metallic properties, while the behavior of the curve itself qualitatively correlates with previous ab initio calculations [5]. We understand that this compound does not actually possess metallic properties, being rather a semiconductor. As the authors note [5], the thin electronic configuration of V3+ leads to ambiguities in the interpretation of the transfer of spin density between atoms in $Li_3V_2(PO_4)_3$. Since such uncertainty may well affect the interpretation of metallic and semiconductor properties, on the one hand, but must remain the same for all supercells to be compared with each other, on the other hand, we accept the resulting cell model as acceptable for our task.

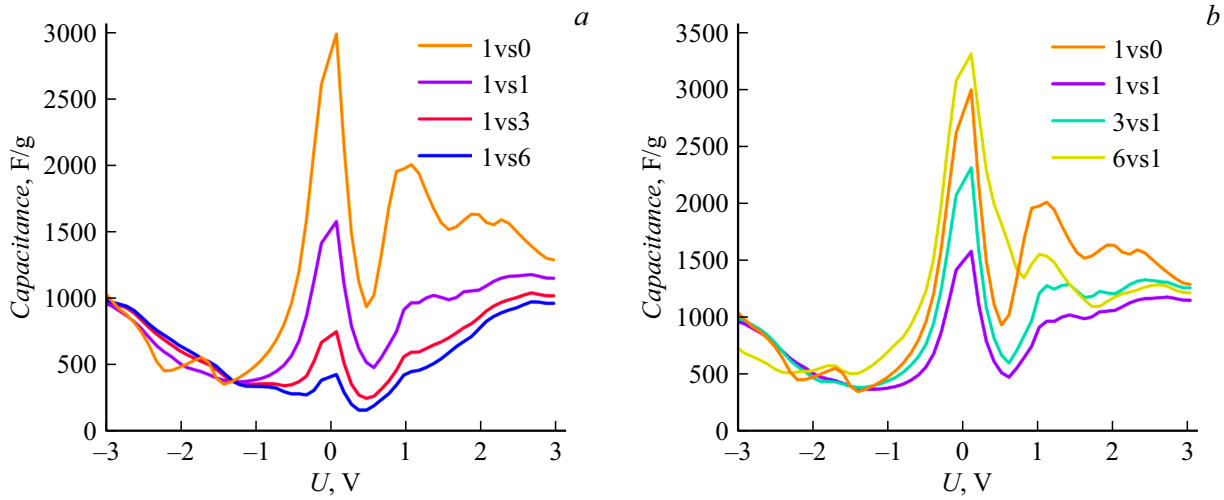

Figure 3. Quantum capacitance of LVP/G composites at various concentrations m($Li_3V_2(PO_4)_3$): m(graphene).

Mass ratio of graphene and cell $Li_3V_2(PO_4)_3$ depending on the number of components, as well as the corresponding Fermi level, quantum capacitance at 0 V and bond energy

m($Li_3V_2(PO_4)_3$): m(graphene)	Quantity graphene cells	Quantity cells $Li_3V_2(PO_4)_3$	$C_Q(0)$, F/g	E_F, eV	E_B, eV
6 : 1	1	2	3184.27	−4.853	−0.253
3 : 1	1	1	2185.96	−4.874	−0.626
1 : 1	3	1	1494.10	−4.858	−1.93
1 : 3	9	1	705.69	−4.989	−1.491
1 : 6	18	1	402.30	−5.089	−1.29

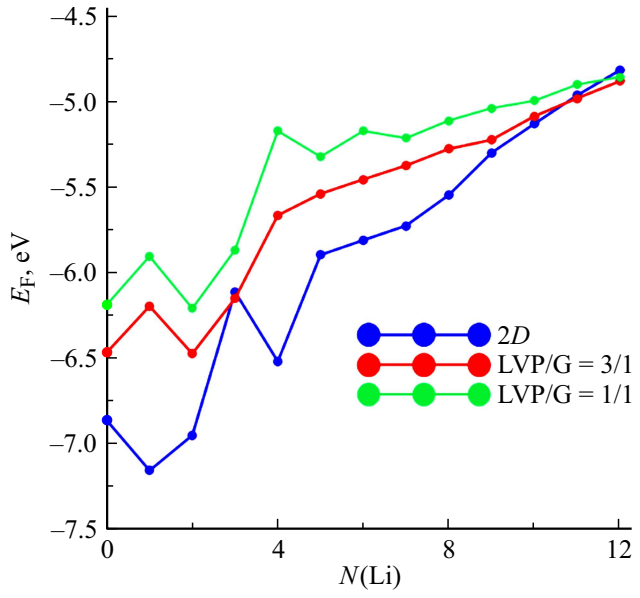

Figure 4. Dependence of the Fermi level on the lithium number in supercells 2*D*-films $Li_3V_2(PO_4)_3$, LVP/G 3 : 1 and LVP/G 1 : 1.

When translating a cell $Li_3V_2(PO_4)_3$ in two directions with Miller indices (1,1,0) (i.e., we are essentially reviewing a 2D film (Fig. 1, *b*)) conductivity at the Fermi level is preserved.

The graphene lattice cell under consideration consisted of 24 carbon atoms. Its dimensions were selected in such a way as to correspond to the translation vectors of the cell $Li_3V_2(PO_4)_3$. The mass ratio of components in the LVP/G composite was varied by the number of graphene layers (from 1 to 18) and the number of cells $Li_3V_2(PO_4)_3$ (from 1 to 2) (see table and Fig. 2). In all cases, the process of composite formation was energetically favorable (bond energies are presented in the table), the main type of interaction being Van der Waals.

The Fermi level values for graphene/$Li_3V_2(PO_4)_3$ composites of these components are in the interval between the Fermi level of pure graphene (−4.528 eV) and 3*D*-cell $Li_3V_2(PO_4)_3$ (−5.160 eV) and are presented in the table. As can be seen from the table, the highest value of the Fermi level (−5.089 eV) is observed in the case when m($Li_3V_2(PO_4)_3$) :m(graphene) = = 1 : 6. This may be due to the fact that the number of graphene cells at a given mass ratio is 18 and we are no longer dealing with graphene, but with a structure close to graphite.

As expected, with an increase in the mass fraction of phosphate in the LVP/G composite, the quantum

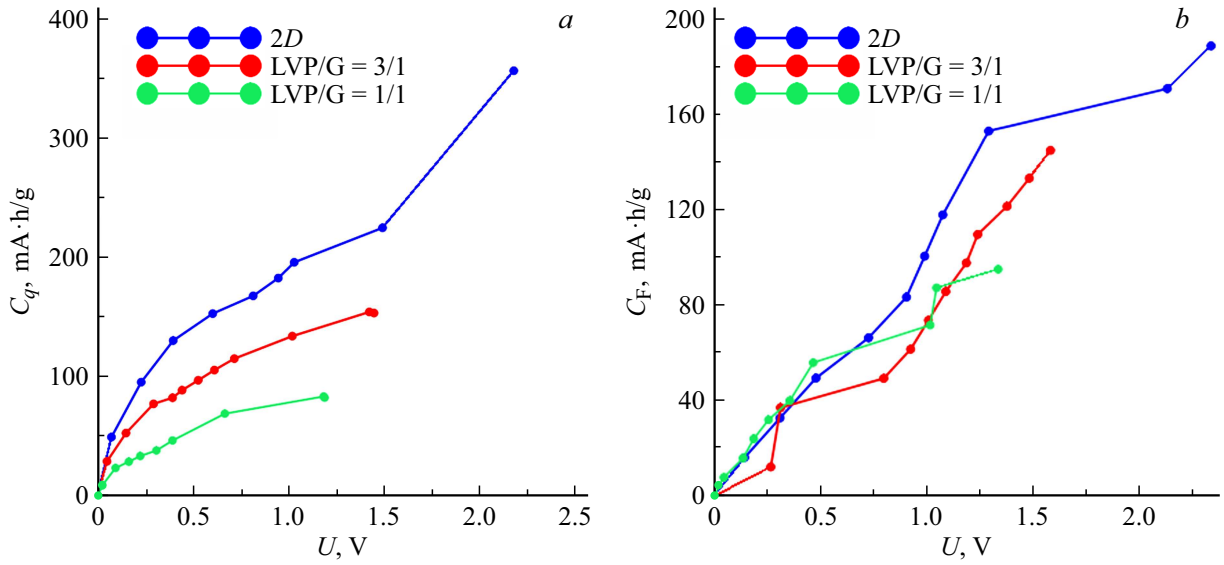

Figure 5. Dependences of quantum and theoretical Faraday capacitance on voltage taking into account changes in the composition of 2*D* films $Li_3V_2(PO_4)_3$, LVP/G 3 : 1 and LVP/G 1 : 1: *a* — quantum capacitance; it b — theoretical Faraday capacity.

capacitance also increases (see table). In the case of concentration $m(Li_3V_2(PO_4)_3)$:m(graphene) = 1 : 6 the value of quantum capacitance at 0 V is 402.30 F/g, 1 : 3 — 705.69 F/g, 1 : 1 — 1494.10 F/g, 3 : 1 — 2185.96 F/g. At the mass ratio 6 : 1, the quantum capacitance at 0 V is equal to 3184.27 F/g, which even exceeds the value of the quantum capacitance at 0 V for the 2*D* film $Li_3V_2(PO_4)_3$ (2799.21 F/g). This is due to the fact that at such a concentration there are two phosphate cells in the composite, and the value of the quantum capacitance at 0 V tends to the value of the 3*D* cell (4631.51 F/g). As can be seen from Fig. 3, the values of quantum capacitance in the range $-3 \le U \le -1$ V are almost identical for all the composites under consideration. There is a maximum at 0 V, which falls as the phosphate concentration decreases. The peak at 1 V, characteristic of the quantum capacitance of pure phosphate, decreases with decreasing phosphate concentration and disappears completely when the mass ratio of the components is equal to 1 : 1.

Next, a series of states was considered during the delithiation of the 2*D* film $Li_3V_2(PO_4)_3$, as well as the $Li_3V_2(PO_4)_3$/graphene) composites with mass ratios $m(Li_3V_2(PO_4)_3)$: m(graphene) 3 : 1 (hereinafter — LVP/G 3 : 1) and 1 : 1 (hereinafter — LVP/G 1 : 1). Each of the presented supercells contains 12 lithium atoms, which were sequentially removed from the structure in the order shown in Fig. 1, *a*. After each removal of a lithium atom, the supercell underwent an optimization process. The dependence of the Fermi level on the number of lithium in the cell is shown in Fig. 4. As can be seen from the figure, the complete filling of supercells with lithium corresponds to almost the same Fermi level, regardless of the presence and concentration of graphene (~ -4.82 eV). This is due to the fact that the Fermi levels of graphene and 2*D*-LVP are approximately at the same energy level. As lithium is extracted, the deviation of the Fermi levels from each other becomes more and more noticeable. With the complete extraction of lithium, the Fermi level of the 2*D* film LVP became equal to — 6.86 eV, for the LVP/G film 3 : 1 — 6.47 eV, for the LVP/G film 1 : 1 — 6.21 eV. If we compare the change in the Fermi level with the voltage drop, we can conclude that with the addition of graphene and an increase in its concentration, the voltage required to extract lithium from the LVP cell decreases. This correlates with the fact that the electrochemical properties of LVP are better realized in the composition of electrode composites with carbon materials [6,7].

A graph of the dependence of quantum capacitance on voltage during the delithiation process is presented in Fig. 5, *a*. The highest quantum capacitance (356.7 mA·h/g) of the electrode is achieved with the 2*D* film of pure $Li_3V_2(PO_4)_3$ at a voltage of 2.19 V. An increase in the mass fraction of graphene leads to a decrease in the maximum quantum capacitance (153.5 mA·h/g in the case of LVP/G 3 : 1 and 82.5 mA·h/g in the case of LVP/G 1 : 1).

The theoretical Faraday capacity can be found using the classical formula:

$$C_F = \frac{N \cdot F}{M \cdot 3.6}, \qquad (5)$$

where N — the amount of lithium in the structure participating in chemical reactions, F — Faraday constant ($9.65 \cdot 10^4$ C/mol), M — mass of the structure. By comparing the amount of extracted lithium with the voltage drop, we obtain the dependence of the Faraday capacity on voltage (Fig. 5, *b*). As can be seen from the figure, the trend observed for the quantum capacitance repeats itself, namely, with increasing graphene concentration, the Faraday capacitance decreases: for the 2*D* film $Li_3V_2(PO_4)_3$ the maximum value of the Faraday capacitance is 197 mA·h/g, for

LVP/G 3 : 1— 146 mA·h/g, for LVP/G1 : 1 — 96 mA·h/g. However, this trend is logical, since in formula (5) the addition of a graphene cell only adds mass to the structure without changing the number of lithium atoms.

Conclusion

What calls attention to itself is the fact that the dependence of the quantum capacitance on voltage obtained as a result of these calculations for materials with a low graphene content significantly exceeds the theoretical values predicted by a simple calculation using Faraday's law. Taking into account the fact that at the electrochemical activity potentials of the proposed cathode material LVP-graphene (3.0−4.7 V relative to metal lithium), only LVP of the components under consideration can exhibit Faraday electrochemical activity, it is very likely that the quantum capacitance is a combination of Faraday and non-Faradaic components, and this combination is represented by a parallel connection. It can be assumed that this non-Faraday component corresponds to the electrical double layer near the surface inside the LVP phase. With an increase in graphene content, another component of the capacitance appears, which is connected in series with the mentioned components, and thereby leads to a decrease in the total capacity. It can be assumed that the last component corresponds to the interfacial double electrical layer. We understand that the mentioned non-Faraday components only include potential charge redistribution within each of the LVP and graphene phases; in the calculations carried out, we do not take into account the presence in a real electrode of another phase of an electrolyte, which, in contact with solid phases, can contribute to the non-Faraday component due to the formation of a double electrical layer with „plates" located as soon as the electrolyte itself, and in different phases.

The resulting shapes of the dependences of quantum capacitance on voltage should correspond to the shapes of the charging curve while maintaining the phase composition, i.e. only with a change in the quantitative content of lithium in the solid solution. Real electrodes based on $Li_3V_2(PO_4)_3$, together with the extraction of lithium, undergo a series of phase transformations. These transformations are reflected by „pads", delays of potentials on the charging and discharge curves. When cycling over a wide range of potentials (3.0−4.7 V relative to metallic lithium), these potentiostatic areas are blurred, the mechanism gradually changes to single-phase [12]. Therefore, we can assume that the resulting graphical dependence of the quantum capacitance on voltage correlates with the charging curve of the Li-based electrode $_3V_2(PO_4)_3$ after several cycles of its charge and discharge. In general, we believe that a successful assessment of the shape of the charging curve of an electrode material has been demonstrated through the analysis of the distributions of differential quantum capacitance over voltage, namely, by taking into account the increments in capacity with increasing voltage, corresponding to the shift in the Fermi level during delithiation.

Funding

The work was funded by the Russian Science Foundation (project № 21-73-10091).

Conflict of interest

The authors declare that they have no conflict of interest.

References

[1] D. Morgan, G. Ceder, M.Y. Saidi, J. Barker, J. Swoyer, H. Huang, G. Adamson. Chem. Mater., **14**, 4684 (2002). DOI: 10.1021/cm020348o
[2] P. Fu, Y. Zhao, Y. Dong, X. Hou. J. Phys. Chem. Solids, **71** (3), 394 (2010). DOI: 10.1016/j.jpcs.2010.01.009
[3] N. Kuganathan, A. Chroneos. Sci. Rep., **9**, 333 (2019). DOI: 10.1038/s41598-018-36398-w
[4] L.S. Cahill, R.P. Chapman, J.F. Britten, G.R. Goward. J. Phys. Chem. B, **110** (14), 7171 (2006). DOI: 10.1021/jp057015+
[5] A. Castets, D. Carlier, K. Trad, C. Delmas, M. Ménétrier. J. Phys. Chem. C, **114** (44), 19141 (2010). DOI: 10.1021/jp106871z
[6] H. Huo, Z. Lin, D. Wu, G. Zhong, J. Shao, X. Xu, B. Xie, Y. Ma, C. Dai, C. Du, P. Zuo, G. Yin. ACS Appl. Energy Mater., **2** (5), 3692 (2019). DOI: 10.1021/acsaem.9b00410
[7] M. Ding, M. Zhao, H. Gong, Q. Zheng, X. Song. Ind. Eng. Chem. Res., **58** (2), 790 (2019). DOI: 10.1021/acs.iecr.8b05150
[8] S. Luryi. Appl. Phys. Lett., **52**, 501 (1988). DOI: 10.1063/1.99649
[9] V. Shunaev, O. Glukhova. Lubricants, **10** (5), 79 (2022). DOI: 10.3390/lubricants10050079
[10] V.V. Shunaev, O.E. Glukhova. Membranes, **11** (8), 642 (2021). DOI: 10.3390/membranes1108064211
[11] J.P. Perdew, K. Burke, M. Ernzerhof. Phys. Rev. Lett., **77** (18), 3865 (1996). DOI: 10.1103/PhysRevLett.77.3865
[12] A.V. Ivanishchev, A.V. Ushakov, I.A. Ivanishcheva, A.V. Churikov, A.V. Mironov, S.S. Fedotov, N.R. Khasanova, E.V. Antipov. Electrochim. Acta, **230**, 479 (2017). DOI: 10.1016/j.electacta.2017.02.009

Translated by A.Akhtyamov